Imaging Advances in Chronic Obstructive Pulmonary Disease

Insights from the Genetic Epidemiology of Chronic Obstructive Pulmonary Disease (COPDGene) Study

Surya P. Bhatt[1], George R. Washko[2], Eric A. Hoffman[3], John D. Newell, Jr.[3], Sandeep Bodduluri[1], Alejandro A. Diaz[2], Craig J. Galban[4], Edwin K. Silverman[5], Raúl San José Estépar[6], and David A. Lynch[7]; for the COPDGene Investigators

[1]UAB Lung Imaging Core and UAB Lung Health Center, Division of Pulmonary, Allergy and Critical Care Medicine, University of Alabama at Birmingham School of Medicine, Birmingham, Alabama; [2]Division of Pulmonary and Critical Care Medicine, [5]Channing Division of Network Medicine, and [6]Department of Radiology, Brigham and Women's Hospital, Harvard Medical School, Boston, Massachusetts; [3]Department of Radiology, University of Iowa Carver College of Medicine, Iowa City, Iowa; [4]Department of Radiology and Center for Molecular Imaging, University of Michigan, Ann Arbor, Michigan; and [7]Department of Radiology, National Jewish Health, Denver, Colorado

ORCID ID: 0000-0002-8418-4497 (S.P.B.).

Abstract

The Genetic Epidemiology of Chronic Obstructive Pulmonary Disease (COPDGene) study, which began in 2007, is an ongoing multicenter observational cohort study of more than 10,000 current and former smokers. The study is aimed at understanding the etiology, progression, and heterogeneity of chronic obstructive pulmonary disease (COPD). In addition to genetic analysis, the participants have been extensively characterized by clinical questionnaires, spirometry, volumetric inspiratory and expiratory computed tomography, and longitudinal follow-up, including follow-up computed tomography at 5 years after enrollment. The purpose of this state-of-the-art review is to summarize the major advances in our understanding of COPD resulting from the imaging findings in the COPDGene study. Imaging features that are associated with adverse clinical outcomes include early interstitial lung abnormalities, visual presence and pattern of emphysema, the ratio of pulmonary artery to ascending aortic diameter, quantitative evaluation of emphysema, airway wall thickness, and expiratory gas trapping. COPD is characterized by the early involvement of the small conducting airways, and the addition of expiratory scans has enabled measurement of small airway disease. Computational advances have enabled indirect measurement of nonemphysematous gas trapping. These metrics have provided insights into the pathogenesis and prognosis of COPD and have aided early identification of disease. Important quantifiable extrapulmonary findings include coronary artery calcification, cardiac morphology, intrathoracic and extrathoracic fat, and osteoporosis. Current active research includes identification of novel quantitative measures for emphysema and airway disease, evaluation of dose reduction techniques, and use of deep learning for phenotyping COPD.

Keywords: chronic obstructive pulmonary disease; lung imaging; computed tomography

Contents

(Received in original form July 21, 2018; accepted in final form October 2, 2018)

Supported by NIH awards U01 HL089897 and U01 HL089856 from NHLBI. S.P.B. is supported by NIH grant K23 HL133438. The content is solely the responsibility of the authors and does not necessarily represent the official views of the NHLBI or the NIH. The COPDGene project is also supported by the COPD Foundation through contributions made to an industry advisory board comprised of AstraZeneca, Boehringer Ingelheim, GlaxoSmithKline, Novartis, Pfizer, Siemens, and Sunovion.

Correspondence and request for reprints should be addressed to Surya P. Bhatt, M.D., Division of Pulmonary, Allergy and Critical Care Medicine, University of Alabama at Birmingham School of Medicine, THT 422, 1720 Second Avenue South, Birmingham, AL 35294. E-mail: sbhatt@uabmc.edu.

This article has an online supplement, which is accessible from this issue's table of contents at www.atsjournals.org.

Am J Respir Crit Care Med Vol 199, Iss 3, pp 286–301, Feb 1, 2019

Originally Published in Press as DOI: 10.1164/rccm.201807-1351SO on October 10, 2018
Internet address: www.atsjournals.org

The Genetic Epidemiology of Chronic Obstructive Pulmonary Disease (COPDGene) study, which began in 2007, is a large multicenter observational cohort study of more than 10,000 current and former smokers, the aim of which is to identify the etiology, progression, and heterogeneity of chronic obstructive pulmonary disease (COPD). Although searching for genetic associations with COPD has been a central goal since the initiation of COPDGene, many other aspects of COPD have been studied as well. With participants undergoing extensive characterization and computed tomographic imaging at two time points approximately 5 years apart, the COPDGene study has served as a rich resource of chest imaging data. The study is ongoing, and further follow-up evaluation of the cohort, including computed tomography (CT), is planned at 10 years after enrollment. More than 80 imaging papers have resulted from the COPDGene study, and these have substantially advanced knowledge of the underlying disease processes. CT complements spirometry, which is a global measure of the presence of disease and adds to disease characterization by providing anatomic localization, differentiating airway disease from emphysema, characterizing emphysema subtypes, and evaluating extrapulmonary manifestations of COPD. Novel quantitative metrics have provided insights into the pathogenesis and prognosis of COPD, and they have aided early identification of disease. Table 1 summarizes the CT metrics developed or tested in COPDGene. Reviews of important imaging findings have recently been published elsewhere (1–3). The purpose of this review is to provide a summary of the most important imaging-related findings resulting from or confirmed in the COPDGene study and to highlight key topics for future imaging research, including early detection of disease, detecting imaging biomarkers for predicting disease progression as well as prediction of exacerbations, and identifying phenotypes for targeted therapy.

COPDGene Cohort

The COPDGene study is an ongoing multicenter cohort study of 10,192 current and former smokers with at least a 10–pack-year smoking history enrolled at 21 centers across the United States (www.clinicaltrials.gov [NCT00608764]) (4). Participants underwent extensive clinical characterization and volumetric CT at baseline (details in the online supplement), and approximately 5,800 returned for a similar follow-up evaluation 5 years later. A 10-year follow-up evaluation is currently being organized. This cohort has a number of unique features that have made it a particularly rich dataset for understanding the imaging features of smoking-related thoracic diseases. Volumetric computed tomographic scans were acquired at full inspiration and end expiration (4). Although spirometric gating was not used for the scans, all participants were coached to full inspiration and end expiration. The cohort enrolled a high number (33%) of African Americans, and approximately half of the subjects had COPD at enrollment. In addition, 457 lifetime nonsmokers were also enrolled as control subjects. Follow-up data on exacerbations and vital status were prospectively obtained via periodic contact (5).

Visual Assessment of Lung Parenchyma

Visual inspection of computed tomographic images provides a qualitative characterization of lung parenchyma and airway disease that is complementary to the global assessment of disease gleaned from spirometry and density-based quantitative measures (Figure 1 and Table 2). Data from COPDGene were analyzed at a workshop of 33 pulmonologists and 25 radiologists to evaluate the agreement in subjective assessment of visual abnormalities between expert readers on a semiquantitative scale and on quantitative measures (6). The concordance between visual and quantitative assessment of emphysema, gas trapping, and bronchial wall thickening was 75%, 87%, and 65%, respectively. Visual subtypes can reliably be estimated at the lobar level with good agreement between readers (7). These observations were instrumental in the development of the Fleischner Society statement on CT-definable subtypes of COPD (8). This statement provides a schema for quantification of visual estimates of disease subtypes, thus allowing comparison across studies. Emphysema classifications include centrilobular (further subclassified as trace, mild, moderate, confluent, and advanced destructive emphysema), panlobular, and paraseptal (further subclassified as mild or substantial) (Table 2). The classification also allows quantification of other abnormalities, including bronchial wall thickening (probable or definite), centrilobular nodules, bronchiectasis, pulmonary arterial enlargement, tracheal abnormalities, and interstitial lung abnormalities (ILAs) (8). Studies from COPDGene have shown that this classification system is useful and correlates with important physiologic and respiratory morbidity outcomes, and visual estimates provide information complementary to quantitative CT for disease characterization (9).

Visual estimates of emphysema are inversely associated with $D_{L_{CO}}$, independent of quantitative emphysema (10). A study of 3,156 COPDGene subjects showed that the presence of any degree of visual emphysema beyond trace is associated with an increased risk of death, even after adjustment for quantitative severity of

Table 1. Summary of Quantitative Metrics for Parenchymal and Airway Disease Based on Computed Tomography Used in the COPDGene Study

Quantitative Metric	Definition	Comments
Bronchial measures		
Segmental or subsegmental bronchial wall thickness	Average thickness of a given airway segment, measured on curved multiplanar reformat	Correlates with increased risk of COPD exacerbation
WA% (34, 35)	Total area of airway − [(area of airway lumen)/total area of airway] × 100	Correlates with physiologic airflow obstruction and with impaired respiratory quality of life
Pi10 (34)	The square root of the wall area of a theoretical airway with internal perimeter 10 mm, derived by plotting the internal perimeters of all measured airways against the square root of the wall area of airways	A useful summary measure of airway wall thickness, adjusted for airway size
Measures of emphysema		
LAA-950	Percentage of lung voxels with CT attenuation less than or equal to −950 HU, measured on inspiratory CT	Correlates with physiologic airflow obstruction and with impaired respiratory quality of life. Several genetic markers have been identified for these measures. May be disproportionately elevated in current cigarette smokers, presumably owing to smoking-related lung inflammation
Perc 15	CT attenuation at the 15th percentile of the lung CT histogram	
Lung mass (27)	Lung mass (g) = [(HU + 1,024)/1,024] × voxel volume × number of voxels	—
Lung density at 15th percentile, corrected for lung volume	Perc 15 converted to lung density in g/L and corrected for baseline total lung volume	Can be used to evaluate progression of emphysema on sequential scans
Local histogram measures	Can be used to estimate the severity of different patterns of emphysema	—
Measures of airway disease		
Excessive central airway collapse (46)	>50% decrease in cross-sectional area of the trachea between inspiration and end expiration	Associated with increased incidence of respiratory exacerbations
LAA-856exp	Percentage of lung voxels with CT attenuation less than or equal to −856 HU measured on expiratory CT scan	Measures of gas trapping; correlate well with physiologic airflow obstruction but do not discriminate between emphysematous and nonemphysematous gas trapping
E/I attenuation ratio (47)	Ratio of mean lung attenuation on expiratory and inspiratory scans	
E/I volume ratio (47)	Ratio of lung volume on expiratory and inspiratory scans	
PRM (50)	Coregistration of inspiratory and expiratory images on a voxel-by-voxel basis to examine the change in density between inspiratory and expiratory images	This method is used to separate gas trapping due to emphysema from gas trapping due to small airways obstruction
PRM^{fSAD} (50)	Percentage of lung voxels with CT attenuation greater than −950 HU on inspiration but less than or equal to −856 HU on expiration on coregistered scans	Measure of nonemphysematous gas trapping, presumed due to small airway obstruction. This is an independent predictor of lung function decline
ND-E/I (49)	Ratio of mean lung density at end expiration to end inspiration in lung voxels with normal density (inspiratory attenuation greater than −910 HU and expiratory attenuation greater than −856 HU)	A potential measure of early small airway disease in lung that would have been classified as normal by traditional metrics
Jacobian determinant (55)	Derived from the deformation of lung volumes at end of respiratory phases to map local volume change between inspiration and expiration	Provides a measure of the level of lung expansion and contraction with respiration
MAL_2 (57)	The percentage of normal voxels within 2-mm distance from emphysematous voxels	Mean Jacobian determinant of these voxels is associated with subsequent FEV_1 decline

(Continued)

Table 1. (*Continued*)

Quantitative Metric	Definition	Comments
Vascular measures		
PA/A ratio (67)	Ratio of the diameter of the pulmonary artery to the diameter of the aorta	An indirect measure of pulmonary hypertension. Correlates with increased frequency of exacerbations of COPD
BV5 (74)	The aggregate blood volume in the small pulmonary vessels <5 mm^2, a measure of pulmonary vascular disease	Correlates with pulmonary vascular pressure
Extrapulmonary measures		
Coronary artery calcification (79)	Agatston-based scoring system	Coronary calcification scoring on nongated scans correlates with gated scores
Osteoporosis (88)	Measurement of bone mineral density on thoracic CT scans	Bone density is substantially reduced in cigarette smokers
Chest wall composition (100)	Automated measurement of pectoralis muscle and subcutaneous fat	Pectoralis area is associated with several indices of COPD severity, including mortality

Definition of abbreviations: COPD = chronic obstructive pulmonary disease; COPDGene = Genetic Epidemiology of Chronic Obstructive Pulmonary Disease; CT = computed tomography; E/I = expiratory/inspiratory; HU = Hounsfield units; LAA = low-attenuation area; MAL_2 = mechanically affected lung within 2 mm of emphysematous voxels; ND-E/I = normal-density E/I; PA/A = pulmonary artery/aorta; Perc 15 = lung attenuation at 15th percentile; PRM = parametric response mapping; PRM^{fSAD} = PRM measure of functional small airway disease; WA% = wall area percentage.

emphysema (11). A further COPDGene paper evaluating the relationship between COPD and lung cancer showed that visually evident emphysema is associated with a 2.3-fold increased risk of future development of lung cancer, but standard quantitative CT measures were not associated with increased risk (12). This discordance between quantitative and visual measurement emphasizes the importance of developing more sensitive and more specific quantitative metrics of emphysema.

COPDGene has led to the increased recognition of a category of smokers who have a preserved FEV_1/FVC ratio but reduced FEV_1 (preserved ratio with impaired spirometry) (13). Compared with subjects with normal spirometry, subjects with preserved ratio with impaired spirometry have increased prevalence of a striking range of comorbidities, including chronic bronchitis, coronary artery disease, diabetes, hypertension, obesity, and gastroesophageal reflux (13). Associated imaging features include a higher frequency of unilateral diaphragm eventration, greater airway wall thickening, centrilobular nodules, reticular abnormalities, paraseptal emphysema, linear atelectasis, kyphosis, and smaller internal transverse thoracic diameter compared with control subjects (14). It is important to recognize these imaging features as contributors to spirometric restriction.

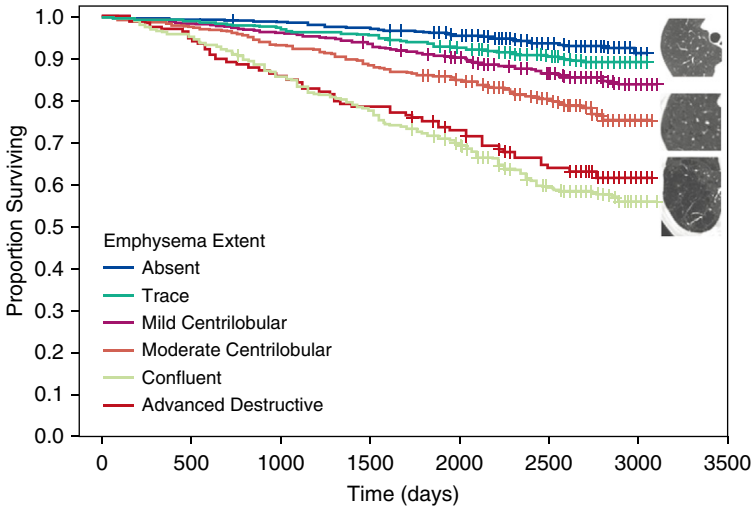

Figure 1. Visual analysis of parenchymal emphysema. Kaplan-Meier survival curves show distinct differences in survival for different emphysema patterns based on the Fleischner Society grading system: the best survival was with absent and trace emphysema (top); those with moderate centrilobular emphysema (center) had intermediate survival; and those with confluent or advanced destructive emphysema (bottom) showed poor survival. These differences persisted after adjustment for potential covariates. Adapted by permission from Reference 11.

Quantitative Phenotyping of Emphysema

Emphysema can be objectively measured by quantifying the fraction of low-attenuation areas of the lung below a selected Hounsfield unit (HU) density threshold. CT abnormalities are found in a substantial proportion of smokers without airflow obstruction, suggesting that the effects of cigarette smoking are substantially underestimated when spirometry alone is relied on for diagnosis; these findings have been confirmed in other cohorts (15, 16). A threshold of -950 HU is the standard

Table 2. Visual Features Evaluated in the COPDGene Study

Visual Metric	Definition	Comments
Centrilobular emphysema (8)	Focal lucencies in the lung, classified as trace, mild centrilobular, moderate centrilobular, confluent, and advanced destructive	Present in up to 44% of cigarette smokers without COPD. Associated with increased risk of mortality and increased risk of lung cancer
Panlobular emphysema	Diffuse decrease in density in the lung, often lower lung predominant	This term is usually reserved for emphysema occurring in patients with known alpha-1 antitrypsin deficiency
Paraseptal emphysema	Subpleural lucencies, classified as mild or substantial	—
Bronchial wall thickening	Subjective thickening of the walls of bronchi, classified as probable or definite	—
Interstitial lung abnormalities (60)	Nondependent abnormalities affecting >5% of any lung zone, including reticular, ground-glass changes, centrilobular nodularity, nonemphysematous cysts, honeycombing, and traction bronchiectasis	Associated with restrictive lung physiology and with increased risk of mortality

Definition of abbreviation: COPD = chronic obstructive pulmonary disease; COPDGene = Genetic Epidemiology of COPD.

accepted threshold, and it has been validated by correlation with histopathology (17, 18). Data from 4,542 COPDGene participants with and without COPD confirmed that quantitative emphysema correlates significantly with both FEV_1/FVC and FEV_1 ($r = -0.76$ and -0.67, respectively) (19). In a separate analysis of 1,200 participants with COPD, quantitative emphysema was associated with respiratory quality of life measured by the St. George's Respiratory Questionnaire (SGRQ) (20). Quantitative emphysema was also associated with the BODE (body mass index, airflow obstruction, dyspnea and exercise capacity) index, a multidimensional score predictive of mortality in patients with COPD, and the effect of emphysema on the BODE score was greater than the effect of airway disease (20, 21). The enrichment of the cohort with African Americans has enabled comparisons of racial differences. In a study of 1,063 subjects with moderate to severe COPD, African Americans had similar lung function impairment compared with non-Hispanic whites, with less CT emphysema but similar airway wall thickness and gas trapping (22). Sex differences also exist for emphysema. Women with early-onset COPD had emphysema similar to that of men despite a markedly lower smoking burden, suggesting greater susceptibility to cigarette smoking in women (23). COPDGene data from normal nonsmoking participants have allowed derivation of normative data for inspiratory and expiratory lung densities by age and sex, as well as normal ranges for lobar densities and lobar size, which may be useful in assessing regional lung dysfunction and response to interventions such as lung volume reduction procedures (24, 25). Sources of variation in density-based measures include inspired lung volume, scanner make and model, increased body mass index (BMI), and increased lung density in individuals who are currently smoking (26, 27). Further information on standardization of density-based measures may be found in the online supplement.

Emphysema quantification using HU density thresholds is based on regional air content. This is influenced by the volume of scan acquisition as well as other processes that affect density, such as active cigarette smoking (26). Recognizing that voxel density is a composite of multiple processes with differing effects on lung density, including the air and tissue content, lung mass was separately calculated in the COPDGene cohort by converting HUs to grams of lung tissue using the following formula: lung mass (in g) = $[(HU + 1{,}024)/1{,}024] \times$ voxel volume $\times$ number of voxels (27). Participants with Global Initiative for Chronic Obstructive Lung Disease (GOLD) spirometry grade 1 had greater lung mass than both smokers with normal lung function and those with GOLD spirometry grades 2 to 4 disease. Although the analysis was cross-sectional, these findings suggest that lung mass changes in COPD are bimodal, with an early increase likely resulting from ongoing lung inflammation and a later decrease resulting from tissue destruction outpacing inflammation (27).

Density threshold–based quantitative CT does not provide information on the visual CT emphysema subtypes, and visual estimation is associated with interrater variability. In COPDGene, regions of interest (ROIs) on inspiratory scans were first labeled in a training dataset, and these labels were used to learn a *k*-nearest neighbor classifier based on location and local histogram-based assessment of lung density that would classify new ROIs into one of six categories (nonemphysematous areas; mild, moderate, and severe centrilobular emphysema; advanced destructive emphysema; and pleura-based emphysema) (Figure 2) (28). Compared with density-based quantitation of overall emphysema, these local histogram-based measures of distinct CT subtypes in COPDGene were associated with lung function, dyspnea, and quality of life. Local histogram-based quantification of pleura-based emphysema also provides a quantification of the risk of pneumothorax (29). Pneumothorax was reported by 3.2% of the participants in the COPDGene cohort, and the risk of past

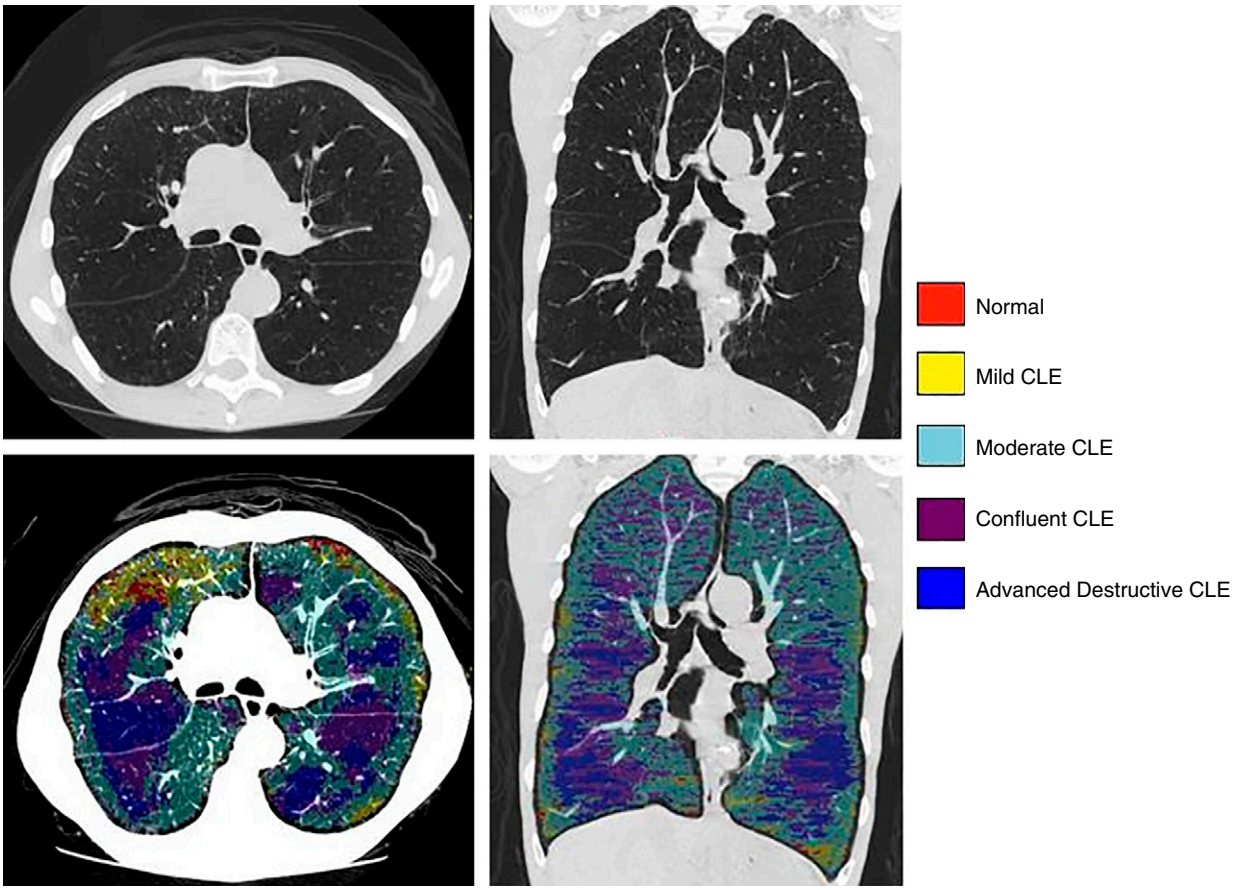

Figure 2. Emphysema subtyping with local histogram. Emphysema subtyping using the local histogram approach for a 61-year-old man with advanced emphysema (low-attenuation area percentage, 38.2%), FEV_1 percent predicted of 26.7%, and body mass index of 16.6 kg/m^2. The top panels show computed tomographic scans for axial and coronal views, and the bottom panels show emphysema subtype labels overlaid on top of the computed tomographic images. Nonemphysematous parenchyma is shown in red, mild centrilobular emphysema (CLE) in yellow, moderate CLE in cyan, confluent CLE in purple, and advanced destructive emphysema in dark blue.

pneumothorax increased by 5% for each 1% increase in pleura-based emphysema.

Quantitative Phenotyping of Airway Disease

Airway disease has historically been measured on the basis of visual inspection, but it is subject to higher interobserver variability than visual measures of emphysema. Newer quantitative tools for airway disease are described below.

Medium and Large Airways

Airflow resistance in COPD arises primarily in the small conducting airways less than 2 mm in diameter, but these airways cannot be visualized with current CT capabilities. The site of these conducting airways varies, and it can range from the 4th to the 12th generations, depending on the size of the individual subject's tracheobronchial tree (30). Based on Weibel's model of airway branching, which states that airways have a dichotomous branching pattern, and assuming that the rate of reduction in lumen size between successive bronchiolar generations is uniform, segmental and subsegmental airway sizes in normal control subjects were used to calculate the projected generation at which the airways were likely to be less than 2 mm in diameter. In normal subjects, this ranged from the 6th to the 10th generations, and this projected branching generation number was significantly associated with FEV_1 independent of lung size and airway lumen size (31). Smaller size of the central airways was associated with lower FEV_1, and those with lower FEV_1 had a lower number of airway generations to reach the small conducting airways. These findings suggest that susceptibility to pathological involvement of conducting airways and hence airflow obstruction might be related to the innate variability of the tracheobronchial tree. As a result of inflammation, COPD is characterized by gradual airway wall thickening and narrowing of lumen, owing to a combination of mucous gland enlargement, smooth muscle hypertrophy, and airway wall fibrosis, a process termed *airway remodeling* (32). Because the inflammation and remodeling processes are thought to arise in the small airways but similarly affect the larger airways, airway remodeling in the segmental and subsegmental airways is used as a surrogate measure of small airway remodeling (33).

A number of metrics are in use to estimate airway size, including direct measures of airway wall thickness and

airway wall area percent [WA% = (total area of airway − area of airway lumen)/total area of airway × 100] (34, 35). Summary measures of airway size are provided by the Pi10 and Pi15, which are the square roots of the wall areas of theoretical airways with internal perimeters of 10 mm and 15 mm, respectively (34). Results from the COPDGene study confirmed that these airway metrics are independently associated with respiratory quality of life measured using SGRQ. When measures were standardized for variability, 1-unit increases in segmental airway wall thickness, WA%, and Pi10 were associated with 1.9-, 1.5-, and 2.8-unit increases in the SGRQ score, respectively (20). These measures of airway thickness are also associated with chronic bronchitis (35), with bronchodilator responsiveness (36), and with a paradoxical response to bronchodilators (37), suggesting that they can predict airway reactivity. These measures can be extracted in a fully automated fashion, thus permitting fast-throughput analysis (38).

Although WA% has strong associations with lung function and respiratory morbidity, it does not provide complete information on the relative remodeling of airway lumen and airway wall. In addition, WA% has a narrow range across the spectrum of normal to severe lung disease, limiting its utility in assessing response to therapy and longitudinal changes over time (39). In an analysis of 5,179 smokers with and without COPD as well as normal control subjects, smokers with the greatest segmental WA% had the greatest degree of airflow obstruction (40). Increases in WA% with progressively greater disease stage were due to a greater reduction in overall airway size with a more modest decrease in wall thickness, suggesting that the increase in WA% with worsening COPD is likely due to a combination of reduced airway size and luminal encroachment by thickened airway walls, findings subsequently confirmed in another large cohort study (41).

The differences in native airway anatomy are also observed as distinct sex differences. Among 2,047 subjects, women had smaller lumen area, smaller internal diameter, and less wall thickness than men in the segmental and subsegmental airways (42). However, the WA% was greater in women than in men. These factors may explain, in part, the sex differences in susceptibility to developing airflow obstruction and COPD (42). Smaller airways are also seen in subjects with a history of childhood asthma, and these subjects are at greater risk of persistent airflow obstruction in adulthood (43).

COPDGene also shed light on the interdependence of airway caliber and lung parenchyma. Airway diameter is expected to increase from end expiration to full inspiration; however, an inverse relationship between airway diameter change with respiration and emphysema was shown, especially in those with emphysema-predominant computed tomographic scans as opposed to airway-predominant computed tomographic scans, and this decrease in airway diameter change was progressively worse with greater airflow obstruction severity grade (44). This might partly explain the lower response to bronchodilators seen in emphysema-predominant disease (45).

In addition to the segmental and subsegmental airways, the large central airways are also involved in smokers, especially those with COPD, owing to either cartilaginous weakening or redundancy of the posterior membranous wall (46). Although expiratory central airway collapse is traditionally diagnosed on the basis of bronchoscopy or using dynamic CT, results from the COPDGene study indicate that expiratory central airway collapse can be identified on dual-volume static computed tomographic scans, which are likely more specific for more severe collapse. In a study of 8,820 subjects, expiratory central airway collapse on CT was present in 5% of all smokers and was more prevalent in those with COPD, and its presence was associated with worse respiratory quality of life as well as a greater frequency of acute respiratory events (46).

Small Airway Abnormality and Expiratory Gas Trapping

With limitations in visualizing small airways directly, gas trapping on expiratory CT has been used as an indirect measure of small airway disease, but this metric is influenced by underlying emphysema (Figure 3). A number of studies using data from the COPDGene study have advanced the capability to estimate small airway disease. The ratio of the expiratory to inspiratory mean lung density (E/I) is an alternative measure of gas trapping that correlates with FEV_1/FVC ($r = -0.62$) and FEV_1 percent predicted ($r = -0.73$) and also with respiratory morbidity indices, including dyspnea, quality of life, and 6-minute-walk distance (47). The E/I ratio of mean lung density correlates with spirometric indices of small airway disease and airway resistance on body plethysmography (48). The E/I ratio may also be applied to areas of the lung that have normal inspiratory and expiratory lung density (greater than −910 HU on inspiration and greater than −856 HU on expiration), and a new metric termed the *normal density E/I* (ND-E/I) was calculated in 8,034 subjects (49). Among smokers without airflow obstruction, 26.3% had ND-E/I above the 90th percentile of normal, and this subthreshold measure that did not meet criteria for mild disease by traditional thresholds was independently associated with FEV_1, SGRQ score, 6-minute-walk distance, and the BODE index, as well as with FEV_1 change on follow-up. These metrics provide a more homogeneous measure of gas trapping adjusted for emphysema, but they do not provide spatial localization of small airway disease.

Parametric response mapping (PRM) is an application of image matching in which inspiratory and expiratory images are deformed and coregistered voxel to voxel, and all voxel pairs are classified on the basis of traditional CT density thresholds for emphysema (50). Voxels that are less than −950 HU on inspiratory CT and less than −856 HU on expiratory CT are termed "emphysematous voxels" (PRM^{Emph}), and voxels that are greater than −950 HU on inspiratory CT and less than −856 HU on expiratory CT are termed "functional small airway disease" (PRM^{fSAD}) and represent areas of nonemphysematous gas trapping (Figure 3). PRM metrics provide spatial information on the distribution of emphysema and small airway disease, thus permitting measurement and tracking of these disease components separately. In a study of 1,508 COPDGene participants, PRM^{fSAD} measured at baseline was associated with subsequent FEV_1 decline in smokers without airflow obstruction as well as in those with early disease, whereas both PRM^{Emph} and PRM^{fSAD} were associated with change in lung function in those with more severe disease (51).

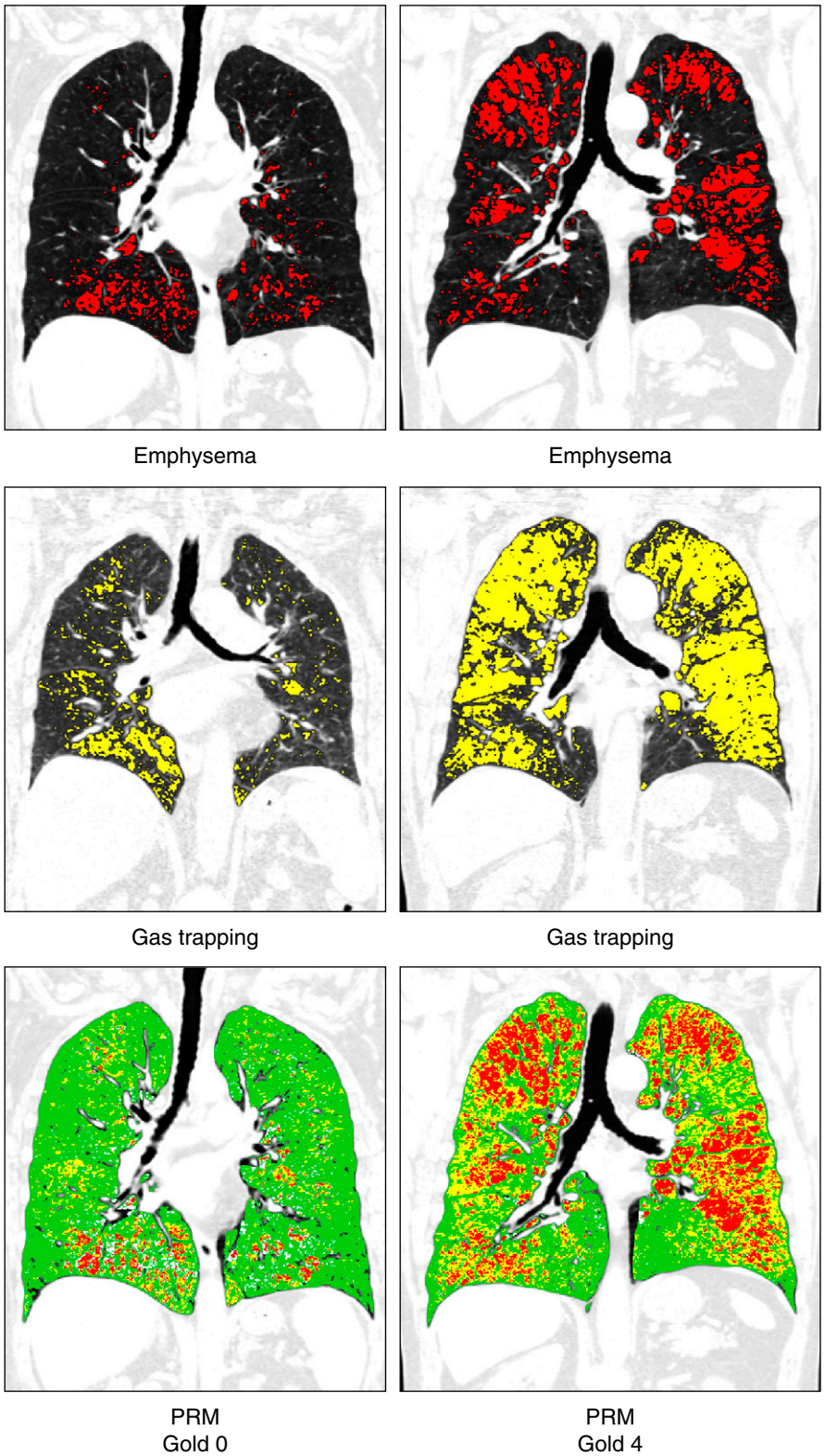

Figure 3. Parametric response mapping (PRM). Top panels show areas of emphysema (low-attenuation area percentages less than −950 Hounsfield units at end inspiration) in red; middle panels show areas of gas trapping (low-attenuation area percentages less than −856 Hounsfield units at end expiration) in yellow; and lower panels show PRM with PRM emphysema voxels in red, PRM functional small airway disease (fSAD) voxels in yellow, and PRM normal voxels in green.

Mechanical and Functional Evaluation of the Lungs

Although CT metrics of emphysema and airway disease correlate with airflow obstruction on spirometry, disease metrics derived from static single-volume computed tomographic scans do not provide complete information on parenchymal abnormalities. In addition to improving spatial localization as described above, lung deformation between inspiration and expiration on image matching can also be used to derive mechanical and functional measures of lung parenchyma. One such metric is the Jacobian determinant, a measure of voxel-level volume change with respiration (52, 53). The Jacobian determinant has values that range from 0 to infinity; values greater than 1 indicate local expansion, values less than 1 imply local contraction, and a value of 1 represents neither local expansion nor contraction. As a measure of regional ventilation, the Jacobian determinant improves the agreement between spirometry and static CT measures of emphysema (54) and is independently associated with SGRQ score, the BODE index, and mortality (55).

COPDGene shed light on the role of the mechanical effects of emphysematous lung on surrounding normal lung in the progression of disease, especially in early disease, whereby alveolar rupture exposes the surrounding normal alveoli to progressively greater mechanical forces, eventually resulting in alveolar rupture (56). The Jacobian determinant was lower not only in the emphysematous areas but also in the normal lung regions (57). This mechanical effect appeared to extend 2 mm out from the emphysematous regions, and the mean Jacobian determinant of this mechanically affected lung within 2 mm of emphysematous lung (MAL_2) was significantly associated with subsequent FEV_1 decline. Quantification of MAL_2 provided a risk estimate for lung function decline, especially in mild to moderate disease, where FEV_1 decline for participants at or above the median MAL_2 was 56 ml/yr compared with 43 ml/yr for those below the median (56).

Importance of Mild ILA

In addition to emphysema, cigarette smoking is associated with fibrotic

and nonfibrotic interstitial lung disease (58). COPDGene has helped to identify the prevalence and importance of ILAs in cigarette smokers without clinical interstitial lung disease who were excluded from the study. An efficient sequential evaluation method to identify and quantify mild ILA was developed using COPDGene computed tomographic scans, and this method had good agreement with existing consensus definitions (Figure 4) (59). ILAs were defined as nondependent abnormalities that affected more than 5% of any lung zone, and they included one or more of reticular, ground-glass changes, centrilobular nodularity, nonemphysematous cysts, honeycombing, and traction bronchiectasis. In a study of 2,416 participants, ILA was detected in 1 in 12 scans, and this finding was associated with lower TLC and a lesser degree of emphysema (60). In a separate analysis of 2,416 smokers, ILA was independently associated with a shorter 6-minute-walk distance, and 82% and 19% of participants with ILA had 6-minute-walk distances less than or equal to 500 m and less than or equal to 250 m, respectively (61). A quantitative analysis of 8,345 participants revealed that a 5% increase in ILA was associated with a 2.5% decrease in FVC percent predicted and a 2.7% reduction in the FEV_1 percent predicted (62). Mortality data were available for 6,827 participants, and a 5% increase in ILA was associated with a 29% increase in mortality risk. The mortality findings with ILAs were confirmed in a large pooled analysis of 11,691 participants from four separate cohorts (63). Between 7% and 9% of participants had ILAs, and over a median follow-up of 3 to 9 years, ILA was associated with increased risk of all-cause mortality in all four cohorts (adjusted hazard ratios ranging from 1.3 to 2.7) (63). Objective approaches have been developed to identify ILAs and may identify clinically and genetically relevant abnormalities even in cases where ILA is not subjectively visible (62, 64, 65).

Predicting Exacerbations

Acute exacerbations of COPD are associated with substantial morbidity, including lower respiratory quality of life, accelerated lung function decline, and increased mortality. The frequency of exacerbations varies quite widely, and predicting acute exacerbations, especially severe exacerbations resulting in hospitalization, can help stratify patients at greatest risk and hence target therapy. In an early analysis of 1,002 participants, bronchial wall thickness and CT emphysema were both associated with the annual rate of exacerbations, such that each 1-mm increase in bronchial wall thickness was associated with a 1.8-fold increase in exacerbation rate (66). A subsequent study examining 3,464 participants with moderate to severe COPD showed that a ratio of the diameter of the pulmonary artery (PA) to the diameter of the aorta (A) greater than 1.0 was associated with a greater frequency of severe exacerbations (odds ratio, 3.44), findings replicated in the ECLIPSE (Evaluation of COPD to Longitudinally Identify Predictive Surrogate Endpoints) cohort (Figure 5) (67). In addition, the presence of expiratory central airway collapse was associated with a 1.5-fold greater frequency of total number of exacerbations and a 1.8-fold increased risk of severe exacerbations (46).

Predicting Progression

A number of CT features predict lung function change over time. Findings from other qualitative and semiquantitative studies that demonstrated an association between the extent of emphysema on CT and subsequent lung function decline were confirmed in COPDGene (51, 68, 69). Among participants with airflow obstruction, every 5% increase in CT emphysema was independently associated with a 3.5 ml/yr additional decline in FEV_1 (51). In a study of 1,623 subjects, lung mass predicted lung function decline such that a 100-g increase in lung mass was associated with a 4.7 ml/yr greater decline in FEV_1, suggesting that inflammatory parenchymal abnormalities precede progression (27). Small airway disease likely precedes emphysema in a substantial proportion of patients with COPD (70, 71). An increase in functional small airway disease (fSAD) by 5% in those with airflow obstruction was associated with a 4.5 ml/yr additional decline in FEV_1, and in those with GOLD 0 disease, fSAD but not emphysema was associated with FEV_1 decline (additional 2.2 ml/yr decline for every 5% increase in fSAD) (Figure 3). The normal density lung E/I ratio (ND-E/I), a measure of small airway disease adjusted for emphysema derived using COPDGene data, was also independently associated with FEV_1 decline (49).

Pulmonary Vascular Disease

Pulmonary hypertension frequently complicates COPD and is often seen in early disease (72). Although definitive diagnosis requires invasive right heart catheterization, chest CT can be used to measure PA enlargement as a surrogate for pulmonary hypertension. A PA/A ratio greater than 1 correlates with pulmonary arterial hypertension and independently predicts future severe exacerbations requiring hospitalization (67). Pulmonary hypertension in COPD is associated with distal vascular pruning in the peripheral regions, and the cross-sectional area of small vessels, less than 5 mm^2 in size, correlates inversely with pulmonary arterial pressure (73). Computational analyses using COPDGene scans have advanced automated segmentation and extraction of the pulmonary vascular tree to enable the automatic calculation of total blood volume and aggregate blood volume in the small vessels less than 5 mm^2 (BV5) in each lobe (Figure 6) (74, 75). Both total blood volume and BV5 correlated inversely with CT emphysema, and after adjustment for age, sex, and emphysema, they were independently associated with resting

Figure 3. (Continued). Representative images are shown for subjects with different stages of disease. The left column shows computed tomographic (CT) images of a 76-year-old woman without airflow obstruction (FEV_1 % predicted, 100%; Global Initiative for Chronic Obstructive Lung Disease [GOLD] stage 0). Quantitative CT density analysis showed 6% emphysema and 19% gas trapping. PRM analysis showed that nonemphysematous gas trapping or fSAD was 13%. The right column shows CT images of a 73-year-old man with GOLD stage 4 (FEV_1 % predicted, 23%), 19% emphysema, and 54% gas trapping. PRM analysis showed that fSAD was 38%.

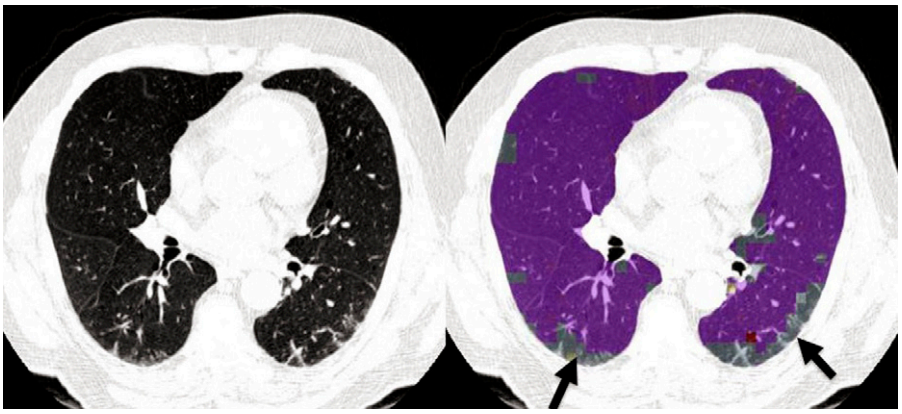

Figure 4. Interstitial lung abnormalities. Images shown are from a 73-year-old male former smoker with FEV_1 percent predicted of 72%, FVC percent predicted of 75%, and no evidence of emphysema by quantitative computed tomographic density analysis (low-attenuation area percentage, 3.2%). Left panel: Computed tomography through the midlungs shows predominantly posterior reticular abnormality. Right panel: Local histogram analysis shows reticular abnormalities outlined in gray (arrows). Purple represents normal lung. Volumetric analysis shows that 11.6% of the lung has reticular abnormalities by the local histogram approach.

oxygen saturation and inversely correlated with SGRQ score and the BODE index (74). By tracing the origin of the small vessels to the hilum, small pulmonary arteries and veins were also separately quantified (76). COPDGene data have been used to develop new computational techniques to separate pulmonary arteries and veins, which may clarify the role of the pulmonary vasculature in the pathogenesis of COPD (77).

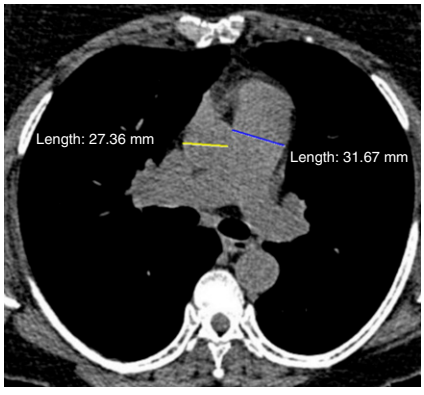

Figure 5. Pulmonary artery/aorta ratio. A 62-year-old smoker with a high frequency of exacerbations ($n = 6$/yr). Computed tomography shows enlarged main pulmonary artery (3.2 cm) with ascending aorta diameter of 2.7 cm (pulmonary artery/aorta ratio, 1.2).

Identification of Extrapulmonary Disease in Smokers

Cardiovascular Disease

There is growing recognition that COPD is associated with a substantial number of comorbidities, many of which share overlapping pathophysiologic pathways. Although CT of the chest is not indicated to evaluate these comorbidities, existing computed tomographic scans lend themselves to assessment of a number of these extrapulmonary manifestations. Cardiovascular disease is two- to fivefold more common in subjects with COPD than in control subjects after adjustment for common cardiac risk factors (78). Coronary artery calcium (CAC) visualized by CT provides diagnostic and prognostic information, and it is commonly quantified using Agatston scores on electrocardiographically gated computed tomographic scans. Given that COPDGene scans were not electrocardiographically gated, 50 participants underwent an additional electrocardiographically gated scan, and there was excellent correlation between CAC scores obtained on gated and nongated protocols (interclass correlation coefficient, 0.96), though the ungated scans did provide a systematically higher estimate of CAC than the gated scans (79). Similar results were reported for thoracic aortic calcification, which provides independent prognostic information for cardiac risk (79). These measures can now be automatically extracted with high accuracy compared with expert detection (80, 81).

Non–ECG-gated scans can also be used to evaluate cardiac morphology. In a study of 24 participants who also had cardiac magnetic resonance imaging and 262 participants with two-dimensional echocardiography, segmentation of the heart and quantification of ventricular volume and sphericity were performed with a statistical model based on nonaffine deformations of the heart to fit the surface of the heart (Figure 7) (82). Cardiac morphometry metrics on CT correlated with both structural and functional measures derived from cardiac magnetic resonance imaging and echocardiography (82). In a separate study of 3,436 participants with moderate to severe COPD followed for 2.1 years, cardiac morphometry was used to predict reduction in exacerbation frequency associated with β-blocker use, especially in those with low left ventricular volume index as well as high right ventricular volume index; a right ventricle/left ventricle ratio of 0.52 can identify participants more likely to respond to β-blocker use (83).

Intra- and Extrathoracic Fat

In addition to estimates of arterial calcification, noncontrast CT can be used to quantify various sources of fat such as epicardial and pericardial fat as well as hepatic fat, all of which are metabolically active, and higher levels are associated with a greater prevalence of diabetes mellitus and subclinical atherosclerosis (79). Abdominal visceral adipose tissue and subcutaneous fat were estimated in 1,267 COPDGene participants, and participants with a history of myocardial infarction had a greater mean visceral adipose tissue area (303.4 ± 208.5 vs. 226.8 ± 172.6 cm^2; $P = 0.002$) than those without a history of myocardial infarction (84). Participants in the highest visceral adipose tissue tertile had a 1.9-fold greater odds of myocardial infarction than those in lower tertiles after adjustment for traditional cardiac risk factors (84).

Cachexia

COPD is also associated with skeletal muscle dysfunction and muscle wasting, and this

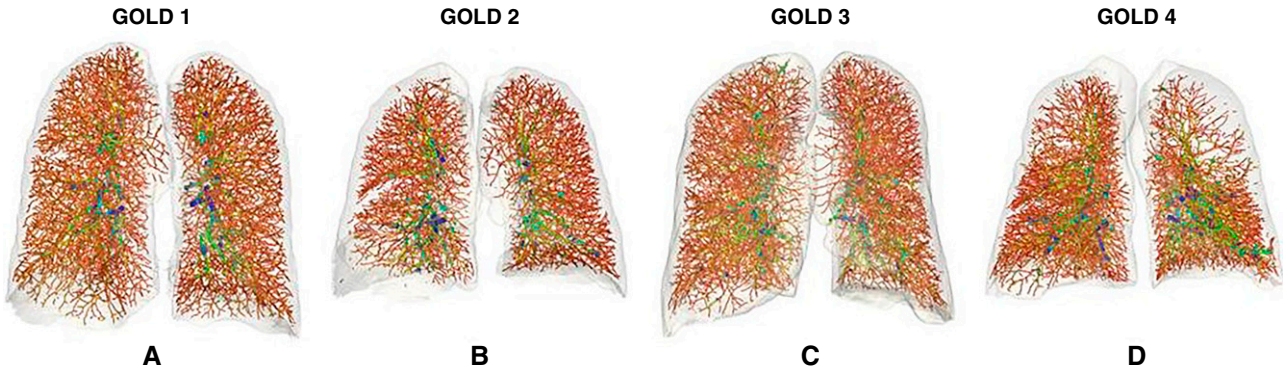

Figure 6. Pulmonary vascular remodeling. Vascular tree rendering showing vascular pruning across Global Initiative for Chronic Obstructive Lung Disease (GOLD) stages. Panels show anterior views of the vascular tree color coded by vessel diameter from small (red to orange) to medium (yellow to green) to large (green to blue) vessels. (*A*) A 58-year-old female current smoker with GOLD stage 1 (FEV_1 % predicted, 85%) with mild emphysema (low-attenuation area percentage [LAA%], 6.0%). The vascular analysis shows a ratio of blood volume for vessels less than 5 mm^2 (BV5) to total blood volume of 0.58 (BV5 was 104.7 ml, and total blood volume was 179.6 ml). (*B*) A 66-year-old female former smoker with GOLD stage 2 (FEV_1 % predicted, 67%) with moderate emphysema (LAA%, 11.3). The vascular analysis shows apparent pruning in the peripheral vasculature with a ratio of BV5 to total blood volume of 0.53 (BV5 was 104.7 ml, and total blood volume was 179.6 ml). (*C*) A 77-year-old male with GOLD stage 3 (FEV_1 % predicted, 30.1%) with mild emphysema (LAA%, 8.5%). The ratio of BV5 to total blood volume is 0.5 (BV5 was 108.8 ml, and total blood volume was 218.2 ml), showing a diffuse vascular pruning. (*D*) A 46-year-old male with GOLD stage 4 (FEV_1 % predicted, 29.3%) with upper lobe emphysema (LAA%, 25.8%). The vascular analysis shows pruning in upper lobes with a ratio of BV5 to total blood volume of 0.46 (BV5 was 104.4 ml, and total blood volume was 227.5 ml).

COPD-related cachexia is not adequately captured by BMI (85). In a study of 966 COPDGene subjects, pectoralis major and minor muscle areas were measured on a single slice at the level of the aortic arch (Figure 8) (86). A new anthropometric measure, the summative pectoralis muscle area, was shown to be associated with fat-free muscle mass and progressively decreased with worsening disease stage. The pectoralis size was more strongly associated than BMI with lung function, dyspnea, and 6-minute-walk distance, and these relationships remained significant after adjustment for BMI (86).

Osteoporosis

COPD is associated with an increased risk of osteoporosis, most likely owing to a multitude of factors, including the use of steroids as well as the systemic inflammation seen in COPD (85). Current guidelines for osteoporosis do not list COPD or cigarette smoking as risk factors (87). CT can be used to estimate bone density, and in a study of 3,321 current and former smokers from COPDGene, a low volumetric bone mineral density (vBMD) was present in 58% of all participants, and 37% had evidence of vertebral fractures (88). The frequency of low vBMD increased with worsening disease stage and was seen in 84% of those with very severe COPD. A notable finding was that male smokers had a higher risk of low vBMD and more fractures than female smokers. These results suggest that radiologists should actively seek evidence of osteopenia and fractures in both male and female smokers.

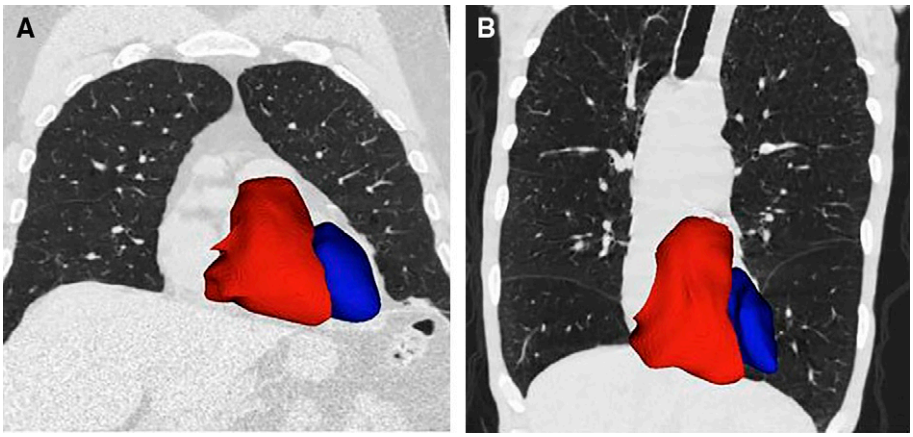

Figure 7. Cardiac remodeling. Computed tomographic images showing left (blue) and right (red) ventricles for two former smokers (anterior view). (*A*) Image of a 73-year-old man with minimal emphysema (low-attenuation area percentage [LAA%], 3.2%); FEV_1 percent predicted of 72.4%; left ventricular (LV) and right ventricular (RV) volumes of 319.1 ml and 183.3 ml, respectively; and RV/LV ratio of 0.57. (*B*) Image of a 61-year-old man with advanced emphysema (LAA%, 38.2%); FEV_1 percent predicted of 26.7%; LV and RV volumes of 208.2 ml and 190.3 ml, respectively; and RV/LV ratio of 0.91.

Computational Advances

Deep Learning and Emerging Artificial Intelligence Techniques

The rich data features in COPDGene lend themselves to the use of artificial intelligence to derive supervised metrics as well as unsupervised or deep learning unbiased metrics for disease quantification and subtyping in an automated fashion.

Supervised learning. Supervised learning is the machine learning task of mapping an input to an output based on examples provided by the investigator. Supervised learning tools have been used in COPDGene to task the machine with identifying emphysema subtypes. The local histogram approach has used labeled ROIs from parenchyma subtypes to quantify the extent of emphysema and interstitial abnormalities (28). Advanced approaches have exploited the use of textural features to quantify emphysema subtypes on the basis of Gabor filters and centrilobular nodularity and centrilobular emphysema using a logistic regression classifier from 50 computer-extracted features (89). Continued smoking is associated with progression in centrilobular emphysema, whereas quitting smoking is associated with a reduction in centrilobular nodularity (89).

Unsupervised learning. In unsupervised learning, the machine is tasked with interpreting input data without the assistance of labeled responses, most commonly by way of identifying clusters or groups of characteristics that tend to form patterns. There is substantial overlap between currently known disease subtypes and cluster analysis of CT data which identifies four subgroups of smokers (relatively resistant smokers, mild upper zone emphysema predominant, airway disease predominant, and severe emphysema) that are reproducible and have strong associations with clinical features as well as distinct and known genetic variants (90). In contrast to previous studies that used supervised classification of ROIs labeled by experts, a generative model has been described that jointly captures heterogeneity of disease subtypes and of the patient population. The disease subtypes identified in this unbiased fashion had stronger associations with FEV_1 and 6-minute-walk distance than those derived from supervised learning (91).

Emergence of deep learning. Deep learning is emerging as a new imaging analysis approach that is currently used across multiple imaging identification problems. Deep learning involves several levels of analysis whereby the machine uses information from the previous level to progressively learn more deeply. Several groups within COPDGene are working on deep learning approaches for automated computed tomographic computation (92–94). COPDGene data have been used to train a convolutional neural network that produces direct detection and staging of COPD and prediction of multiple COPDGene outcomes, including acute respiratory events and mortality. Convolutional neural networks, rather than focusing on one specific aspect of the image, integrate the whole of the imaging information. These results were independently replicated in ECLIPSE using the models trained in COPDGene, suggesting the robustness of the models. Nevertheless, this is an emerging field, and more technical development is needed to be able to process entire three-dimensional scans.

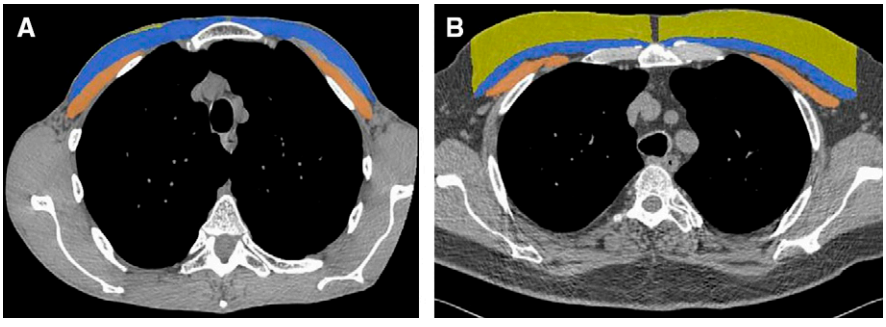

Figure 8. Body composition phenotypes. Manual segmentation of pectoralis muscles (blue = pectoralis major; brown = pectoralis minor) and subcutaneous adipose tissue (yellow) at the level of the aortic arch. (*A*) Image of a 62-year-old former smoker with body mass index of 16.6 kg/m^2, 37% emphysema based on computed tomography, and FEV_1 percent predicted of 27%. The cross-sectional area is 3,488 mm^2 for the pectoralis muscles and 176 mm^2 for the subcutaneous fat. (*B*) Image of a 61-year-old former smoker with body mass index of 30 kg/m^2, 11% emphysema, and FEV_1 percent predicted of 78%. The cross-sectional area is 3,545 mm^2 for the pectoralis muscles and 7,533 mm^2 for subcutaneous fat.

Relationship between Imaging and Genetics

Identifying genetic determinants of complex diseases such as COPD has been transformed by the availability, at reasonable cost and high accuracy, of genome-wide panels of hundreds of thousands of genetic variants (known as *single-nucleotide polymorphisms*, or "SNPs") that capture most of the common variation in the human genome. Genome-wide panels of genetic variants have been tested for statistical association with many complex diseases and disease-related phenotypes, and thousands of associations remain statistically significant despite the substantial adjustment for multiple statistical testing that is performed in genome-wide association studies (GWAS), typically requiring $P < 5E\text{-}8$ (95). Combining association evidence from multiple collaborative studies is often required to obtain adequate power in GWAS. Although GWAS have been quite successful at identifying regions of the genome related to complex diseases, follow-up studies within those regions are required to identify the key genes and their functional genetic variants.

The rich imaging phenotypes in COPDGene have enabled multiple successful genetic association studies. In a collaborative study with ECLIPSE, GenKOLS (Genetics of COPD, Norway), and NETT (National Emphysema Treatment Trial), five genome-wide significant regions with densitometric emphysema at −950 HU were found, including several regions associated with COPD (*HHIP*, *CHRNA3/CHRNA5*, and *AGER*), a novel region near *DLC1*, and the alpha-1 antitrypsin (*SERPINA1*) region (96). Visual assessments of emphysema and airway disease in COPDGene have been associated with genetic loci that were previously associated with susceptibility to COPD or with quantitative computed tomographic measures, suggesting that genetic associations for visual estimates and quantitative CT are reproducible (9). Genome-wide significant associations have also been identified for emphysema distribution (97), local histogram emphysema pattern (98), and PA/A ratio (99). With each of these imaging phenotypes, some previously identified COPD-associated loci have been confirmed, and new genetic loci have been discovered. Thus, we anticipate that

there will be both shared genetic determinants for COPD susceptibility that influence imaging-based phenotypes as well as specific genetic determinants for those imaging phenotypes.

Translating these advances in the genetics of imaging phenotypes to more specific diagnosis and treatment of patients with COPD remains a major challenge. However, unbiased genetic approaches to uncover pathobiological determinants of imaging phenotypes could identify key contributors to the heterogeneous imaging patterns of COPD and new molecular targets for pharmacological treatment development in specific subtypes of COPD.

Future Directions

The rich dataset of computed tomographic images from a large number of clinically and spirometrically well-characterized subjects in the COPDGene cohort opens new avenues for research in the future. These will include assessment of longitudinal change in the phenotypes described in the earlier sections, as well as integration of omics data such as gene expression, protein biomarkers, and metabolomics with imaging phenotypes. These studies will improve knowledge of the relationship between structural, functional, and biological changes that occur in COPD. Although there is no therapy that is currently informed by imaging-based phenotyping except lung volume reduction procedures, we anticipate that imaging research will result in robust biomarkers for early detection of disease, for predicting disease progression, and for prediction of exacerbations. Future research will also focus on imaging-based phenotypes of emphysema and small airway disease that will enable targeted therapy in COPD.

Conclusions

Data from COPDGene and other large cohorts provide insight into the disease processes involved and add considerable information to that obtained by spirometry (Figure 9). Studies from COPDGene have advanced awareness in a number of areas, including early identification of disease; recognition of symptomatic smokers without airflow obstruction; the importance of mild interstitial abnormalities in smokers; and measurement of extrapulmonary comorbidities, including coronary artery disease, pulmonary vascular disease, cachexia, and osteoporosis. In those at risk for or with established early disease, CT provides robust risk estimates for important respiratory outcomes, including quality of life, dyspnea, exercise capacity, exacerbations, lung function decline, and mortality, over and beyond that derived from spirometric measures. With rapid advances being made in the acquisition of reduced-dose CT without compromising image quality, CT will likely be an important tool in the diagnosis and management of patients with COPD. These advances will be hastened by the use of reduced-dose CT scans for the 10-year follow-up scans in phase 3 of the COPDGene study. ■

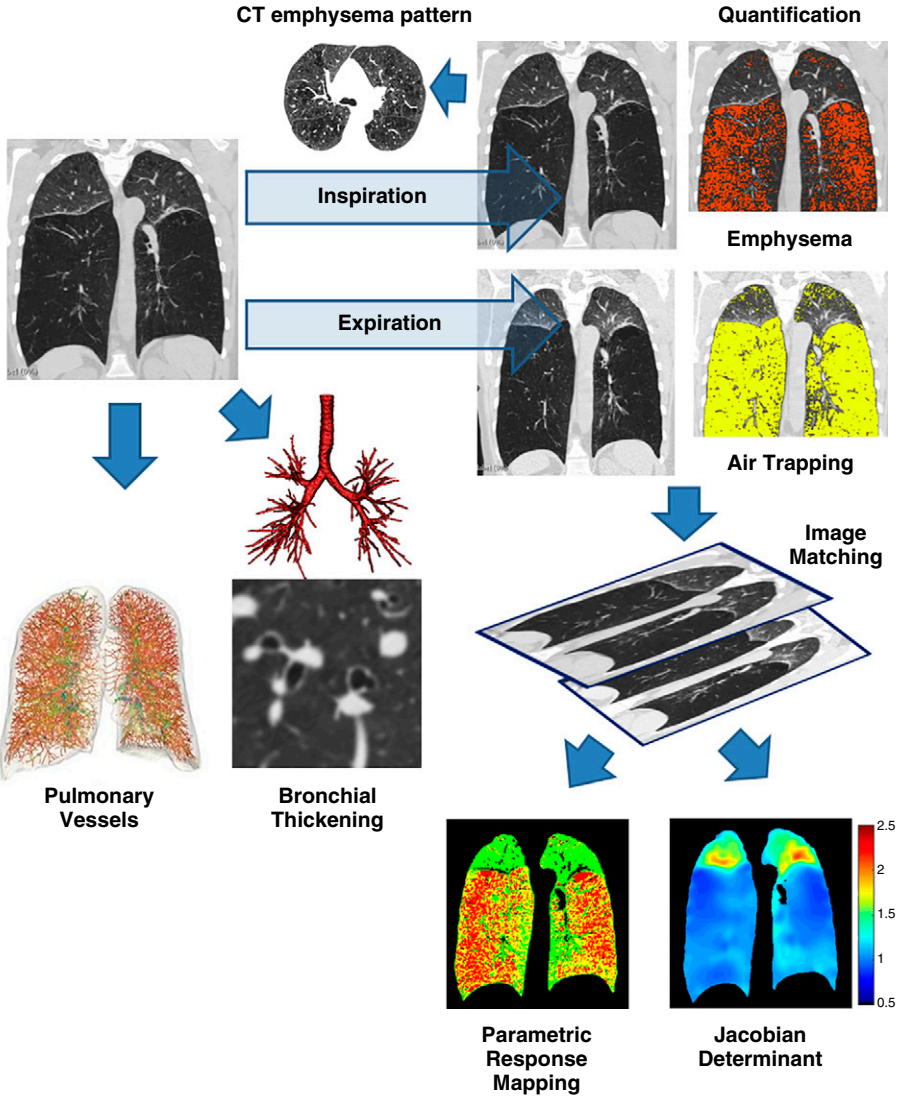

Figure 9. Summary of imaging features that can be derived from computed tomography (CT). The figure shows a summary of the main measurements that can be made using inspiratory computed tomographic scans. These include qualitative and semiquantitative determination of emphysema and emphysema subtype, quantitative estimates of emphysema using density histograms, bronchial wall thickness, and pulmonary vasculature. The addition of expiratory scans enables image matching and the computation of functional small airway disease using parametric response mapping, as well as the Jacobian determinant, an estimate of lung mechanics.

Author disclosures are available with the text of this article at www.atsjournals.org.

Acknowledgment: The authors sincerely acknowledge the contributions to this review of MeiLan K. Han, M.D.; Sean B. Fain, Ph.D.; Stephen Humphries, Ph.D.; Francine L. Jacobson, M.D.; and Charles R. Hatt, Ph.D.

References

1. Kirby M, van Beek EJR, Seo JB, Biederer J, Nakano Y, Coxson HO, *et al*. Management of COPD: is there a role for quantitative imaging? *Eur J Radiol* 2017;86:335–342.
2. Labaki WW, Martinez CH, Martinez FJ, Galbán CJ, Ross BD, Washko GR, *et al*. The role of chest computed tomography in the evaluation and management of the patient with chronic obstructive pulmonary disease. *Am J Respir Crit Care Med* 2017;196:1372–1379.
3. Bodduluri S, Reinhardt JM, Hoffman EA, Newell JD Jr, Bhatt SP. Recent advances in computed tomography imaging in chronic obstructive pulmonary disease. *Ann Am Thorac Soc* 2018;15:281–289.
4. Regan EA, Hokanson JE, Murphy JR, Make B, Lynch DA, Beaty TH, *et al*. Genetic Epidemiology of COPD (COPDGene) study design. *COPD* 2010;7:32–43.
5. Stewart JI, Moyle S, Criner GJ, Wilson C, Tanner R, Bowler RP, *et al*.; for the COPDGene Investigators. Automated telecommunication to obtain longitudinal follow-up in a multicenter cross-sectional COPD study. *COPD* 2012;9:466–472.
6. Barr RG, Berkowitz EA, Bigazzi F, Bode F, Bon J, Bowler RP, *et al*.; COPDGene CT Workshop Group. A combined pulmonary-radiology workshop for visual evaluation of COPD: study design, chest CT findings and concordance with quantitative evaluation. *COPD* 2012;9: 151–159.
7. Kim SS, Seo JB, Lee HY, Nevrekar DV, Forssen AV, Crapo JD, *et al*. Chronic obstructive pulmonary disease: lobe-based visual assessment of volumetric CT by using standard images—comparison with quantitative CT and pulmonary function test in the COPDGene study. *Radiology* 2013; 266:626–635.
8. Lynch DA, Austin JH, Hogg JC, Grenier PA, Kauczor HU, Bankier AA, *et al*. CT-definable subtypes of chronic obstructive pulmonary disease: a statement of the Fleischner Society. *Radiology* 2015;277: 192–205.
9. Halper-Stromberg E, Cho MH, Wilson C, Nevrekar D, Crapo JD, Washko G, *et al*. Visual assessment of chest computed tomographic images is independently useful for genetic association analysis in studies of chronic obstructive pulmonary disease. *Ann Am Thorac Soc* 2017;14:33–40.
10. Nambu A, Zach J, Schroeder J, Jin GY, Kim SS, Kim YI, *et al*. Relationships between diffusing capacity for carbon monoxide (DLCO), and quantitative computed tomography measurements and visual assessment for chronic obstructive pulmonary disease. *Eur J Radiol* 2015;84:980–985.
11. Lynch DAMC, Moore CM, Wilson C, Nevrekar D, Jennermann T, Humphries SM, *et al*.; Genetic Epidemiology of COPD (COPDGene) Investigators. CT-based visual classification of emphysema: association with mortality in the COPDGene Study. *Radiology* 2018; 288:859–866.
12. Carr LL, Jacobson S, Lynch DA, Foreman MG, Flenaugh EL, Hersh CP, *et al*. Features of COPD as predictors of lung cancer. *Chest* 2018; 153:1326–1335.
13. Wan ES, Hokanson JE, Murphy JR, Regan EA, Make BJ, Lynch DA, *et al*.; COPDGene Investigators. Clinical and radiographic predictors of GOLD-unclassified smokers in the COPDGene study. *Am J Respir Crit Care Med* 2011;184:57–63.
14. Kim SS, Yagihashi K, Stinson DS, Zach JA, McKenzie AS, Curran-Everett D, *et al*. Visual assessment of CT findings in smokers with nonobstructed spirometric abnormalities in the COPDGene® Study. *Chronic Obstr Pulm Dis* 2014;1:88–96.
15. Regan EA, Lynch DA, Curran-Everett D, Curtis JL, Austin JH, Grenier PA, *et al*. .; Genetic Epidemiology of COPD (COPDGene) Investigators. Clinical and radiologic disease in smokers with normal spirometry. *JAMA Intern Med* 2015;175:1539–1549.
16. Woodruff PG, Barr RG, Bleecker E, Christenson SA, Couper D, Curtis JL, *et al*.; SPIROMICS Research Group. Clinical significance of symptoms in smokers with preserved pulmonary function. *N Engl J Med* 2016;374:1811–1821.
17. Madani A, De Maertelaer V, Zanen J, Gevenois PA. Pulmonary emphysema: radiation dose and section thickness at multidetector CT quantification—comparison with macroscopic and microscopic morphometry. *Radiology* 2007;243:250–257.
18. Gevenois PA, de Maertelaer V, De Vuyst P, Zanen J, Yernault JC. Comparison of computed density and macroscopic morphometry in pulmonary emphysema. *Am J Respir Crit Care Med* 1995;152: 653–657.
19. Schroeder JD, McKenzie AS, Zach JA, Wilson CG, Curran-Everett D, Stinson DS, *et al*. Relationships between airflow obstruction and quantitative CT measurements of emphysema, air trapping, and airways in subjects with and without chronic obstructive pulmonary disease. *AJR Am J Roentgenol* 2013;201:W460–W470.
20. Martinez CH, Chen YH, Westgate PM, Liu LX, Murray S, Curtis JL, *et al*.; COPDGene Investigators. Relationship between quantitative CT metrics and health status and BODE in chronic obstructive pulmonary disease. *Thorax* 2012;67:399–406.
21. Celli BR, Cote CG, Marin JM, Casanova C, Montes de Oca M, Mendez RA, *et al*. The body-mass index, airflow obstruction, dyspnea, and exercise capacity index in chronic obstructive pulmonary disease. *N Engl J Med* 2004;350:1005–1012.
22. Hansel NN, Washko GR, Foreman MG, Han MK, Hoffman EA, DeMeo DL, *et al*.; COPDGene Investigators. Racial differences in CT phenotypes in COPD. *COPD* 2013;10:20–27.
23. Hardin M, Foreman M, Dransfield MT, Hansel N, Han MK, Cho MH, *et al*.; COPDGene Investigators. Sex-specific features of emphysema among current and former smokers with COPD. *Eur Respir J* 2016; 47:104–112.
24. Come CE, Diaz AA, Curran-Everett D, Muralidhar N, Hersh CP, Zach JA, *et al*.; COPDGene Investigators. Characterizing functional lung heterogeneity in COPD using reference equations for CT scan-measured lobar volumes. *Chest* 2013;143:1607–1617.
25. Zach JA, Newell JD Jr, Schroeder J, Murphy JR, Curran-Everett D, Hoffman EA, *et al*.; COPDGene Investigators. Quantitative computed tomography of the lungs and airways in healthy nonsmoking adults. *Invest Radiol* 2012;47:596–602.
26. Zach JA, Williams A, Jou SS, Yagihashi K, Everett D, Hokanson JE, *et al*.; COPDGene Investigators. Current smoking status is associated with lower quantitative CT measures of emphysema and gas trapping. *J Thorac Imaging* 2016;31:29–36.
27. Washko GR, Kinney GL, Ross JC, San José Estépar R, Han MK, Dransfield MT, *et al*.; COPDGene Investigators. Lung mass in smokers. *Acad Radiol* 2017;24:386–392.
28. Castaldi PJ, San José Estépar R, Mendoza CS, Hersh CP, Laird N, Crapo JD, *et al*. Distinct quantitative computed tomography emphysema patterns are associated with physiology and function in smokers. *Am J Respir Crit Care Med* 2013;188: 1083–1090.
29. Hobbs BD, Foreman MG, Bowler R, Jacobson F, Make BJ, Castaldi PJ, *et al*.; COPDGene Investigators. Pneumothorax risk factors in smokers with and without chronic obstructive pulmonary disease. *Ann Am Thorac Soc* 2014;11:1387–1394.
30. Hogg JC, Chu F, Utokaparch S, Woods R, Elliott WM, Buzatu L, *et al*. The nature of small-airway obstruction in chronic obstructive pulmonary disease. *N Engl J Med* 2004;350:2645–2653.
31. Diaz AA, Rahaghi FN, Ross JC, Harmouche R, Tschirren J, San José Estépar R, *et al*.; COPD Gene investigators. Understanding the contribution of native tracheobronchial structure to lung function: CT assessment of airway morphology in never smokers. *Respir Res* 2015;16:23.
32. Aoshiba K, Nagai A. Differences in airway remodeling between asthma and chronic obstructive pulmonary disease. *Clin Rev Allergy Immunol* 2004;27:35–43.
33. Nakano Y, Wong JC, de Jong PA, Buzatu L, Nagao T, Coxson HO, *et al*. The prediction of small airway dimensions using computed tomography. *Am J Respir Crit Care Med* 2005;171:142–146.
34. Grydeland TB, Dirksen A, Coxson HO, Eagan TM, Thorsen E, Pillai SG, *et al*. Quantitative computed tomography measures of emphysema and airway wall thickness are related to respiratory symptoms. *Am J Respir Crit Care Med* 2010;181:353–359.
35. Kim V, Davey A, Comellas AP, Han MK, Washko G, Martinez CH, *et al*.; COPDGene® Investigators. Clinical and computed tomographic predictors of chronic bronchitis in COPD: a cross sectional analysis of the COPDGene Study. *Respir Res* 2014;15:52.

36. Kim V, Desai P, Newell JD, Make BJ, Washko GR, Silverman EK, *et al*.; COPDGene Investigators. Airway wall thickness is increased in COPD patients with bronchodilator responsiveness. *Respir Res* 2014;15:84.
37. Bhatt SP, Wells JM, Kim V, Criner GJ, Hersh CP, Hardin M, *et al*.; COPDGene Investigators. Radiological correlates and clinical implications of the paradoxical lung function response to β_2 agonists: an observational study. *Lancet Respir Med* 2014;2: 911–918.
38. Estépar RS, Ross JC, Kindlmann GL, Diaz A, Okajima Y, Kikinis R, *et al*. Automatic airway analysis for genome-wide association studies in COPD. *Proc IEEE Int Symp Biomed Imaging* 2012:1467–1470.
39. Coxson HO, Quiney B, Sin DD, Xing L, McWilliams AM, Mayo JR, *et al*. Airway wall thickness assessed using computed tomography and optical coherence tomography. *Am J Respir Crit Care Med* 2008; 177:1201–1206.
40. Washko GR, Diaz AA, Kim V, Barr RG, Dransfield MT, Schroeder J, *et al*. Computed tomographic measures of airway morphology in smokers and never-smoking normals. *J Appl Physiol (1985)* 2014; 116:668–673.
41. Smith BM, Hoffman EA, Rabinowitz D, Bleecker E, Christenson S, Couper D, *et al*.; The Multi-Ethnic Study of Atherosclerosis (MESA) COPD Study and the Subpopulations and Intermediate Outcomes in COPD Study (SPIROMICS). Comparison of spatially matched airways reveals thinner airway walls in COPD. *Thorax* 2014;69: 987–996.
42. Kim YI, Schroeder J, Lynch D, Newell J, Make B, Friedlander A, *et al*.; COPDGene Investigators. Gender differences of airway dimensions in anatomically matched sites on CT in smokers. *COPD* 2011;8:285–292.
43. Diaz AA, Hardin ME, Come CE, San José Estépar R, Ross JC, Kurugol S, *et al*.; COPDGene Investigators. Childhood-onset asthma in smokers: association between CT measures of airway size, lung function, and chronic airflow obstruction. *Ann Am Thorac Soc* 2014; 11:1371–1378.
44. Diaz AA, Come CE, Ross JC, San José Estépar R, Han MK, Loring SH, *et al*.; COPDGene Investigators. Association between airway caliber changes with lung inflation and emphysema assessed by volumetric CT scan in subjects with COPD. *Chest* 2012;141:736–744.
45. Han MK, Wise R, Mumford J, Sciurba F, Criner GJ, Curtis JL, *et al*.; NETT Research Group. Prevalence and clinical correlates of bronchoreversibility in severe emphysema. *Eur Respir J* 2010;35: 1048–1056.
46. Bhatt SP, Terry NL, Nath H, Zach JA, Tschirren J, Bolding MS, *et al*.; Genetic Epidemiology of COPD (COPDGene) Investigators. Association between expiratory central airway collapse and respiratory outcomes among smokers. *JAMA* 2016;315:498–505.
47. Hersh CP, Washko GR, Estépar RS, Lutz S, Friedman PJ, Han MK, *et al*.; COPDGene Investigators. Paired inspiratory-expiratory chest CT scans to assess for small airways disease in COPD. *Respir Res* 2013;14:42.
48. Nambu A, Zach J, Schroeder J, Jin G, Kim SS, Kim YI, *et al*. Quantitative computed tomography measurements to evaluate airway disease in chronic obstructive pulmonary disease: relationship to physiological measurements, clinical index and visual assessment of airway disease. *Eur J Radiol* 2016;85:2144–2151.
49. Bodduluri S, Reinhardt JM, Hoffman EA, Newell JD Jr, Nath H, Dransfield MT, *et al*.; COPDGene Investigators. Signs of gas trapping in normal lung density regions in smokers. *Am J Respir Crit Care Med* 2017;196:1404–1410.
50. Galbán CJ, Han MK, Boes JL, Chughtai KA, Meyer CR, Johnson TD, *et al*. Computed tomography-based biomarker provides unique signature for diagnosis of COPD phenotypes and disease progression. *Nat Med* 2012;18:1711–1715.
51. Bhatt SP, Soler X, Wang X, Murray S, Anzueto AR, Beaty TH, *et al*.; COPDGene Investigators. Association between functional small airway disease and FEV_1 decline in chronic obstructive pulmonary disease. *Am J Respir Crit Care Med* 2016;194:178–184.
52. Reinhardt JM, Christensen GE, Hoffman EA, Ding K, Cao K. Registration-derived estimates of local lung expansion as surrogates for regional ventilation. *Inf Process Med Imaging* 2007;20:763–774.
53. Bodduluri S, Newell JD Jr, Hoffman EA, Reinhardt JM. Registration-based lung mechanical analysis of chronic obstructive pulmonary disease (COPD) using a supervised machine learning framework. *Acad Radiol* 2013;20:527–536.
54. Bhatt SP, Bodduluri S, Newell JD, Hoffman EA, Sieren JC, Han MK, *et al*.; COPDGene Investigators. CT-derived biomechanical metrics improve agreement between spirometry and emphysema. *Acad Radiol* 2016;23:1255–1263.
55. Bodduluri S, Bhatt SP, Hoffman EA, Newell JD Jr, Martinez CH, Dransfield MT, *et al*.; COPDGene Investigators. Biomechanical CT metrics are associated with patient outcomes in COPD. *Thorax* 2017; 72:409–414.
56. Ritter MC, Jesudason R, Majumdar A, Stamenovic D, Buczek-Thomas JA, Stone PJ, *et al*. A zipper network model of the failure mechanics of extracellular matrices. *Proc Natl Acad Sci USA* 2009;106:1081–1086.
57. Bhatt SP, Bodduluri S, Hoffman EA, Newell JD Jr, Sieren JC, Dransfield MT, *et al*.; COPDGene Investigators. Computed tomography measure of lung at risk and lung function decline in chronic obstructive pulmonary disease. *Am J Respir Crit Care Med* 2017; 196:569–576.
58. Jin GY, Lynch D, Chawla A, Garg K, Tammemagi MC, Sahin H, *et al*. Interstitial lung abnormalities in a CT lung cancer screening population: prevalence and progression rate. *Radiology* 2013;268: 563–571.
59. Washko GR, Lynch DA, Matsuoka S, Ross JC, Umeoka S, Diaz A, *et al*. Identification of early interstitial lung disease in smokers from the COPDGene Study. *Acad Radiol* 2010;17:48–53.
60. Washko GR, Hunninghake GM, Fernandez IE, Nishino M, Okajima Y, Yamashiro T, *et al*.; COPDGene Investigators. Lung volumes and emphysema in smokers with interstitial lung abnormalities. *N Engl J Med* 2011;364:897–906.
61. Doyle TJ, Washko GR, Fernandez IE, Nishino M, Okajima Y, Yamashiro T, *et al*.; COPDGene Investigators. Interstitial lung abnormalities and reduced exercise capacity. *Am J Respir Crit Care Med* 2012;185: 756–762.
62. Ash SY, Harmouche R, Putman RK, Ross JC, Diaz AA, Hunninghake GM, *et al*.; COPDGene Investigators. Clinical and genetic associations of objectively identified interstitial changes in smokers. *Chest* 2017;152: 780–791.
63. Putman RK, Hatabu H, Araki T, Gudmundsson G, Gao W, Nishino M, *et al*.; Evaluation of COPD Longitudinally to Identify Predictive Surrogate Endpoints (ECLIPSE) Investigators; COPDGene Investigators. Association between interstitial lung abnormalities and all-cause mortality. *JAMA* 2016;315:672–681.
64. Ash SY, Harmouche R, Ross JC, Diaz AA, Hunninghake GM, Putman RK, *et al*. The objective identification and quantification of interstitial lung abnormalities in smokers. *Acad Radiol* 2017;24: 941–946.
65. Ash SY, Harmouche R, Ross JC, Diaz AA, Rahaghi FN, Vegas Sanchez-Ferrero G, *et al*.; COPDGene Investigators. Interstitial features modify the effects of emphysema in the COPDGene cohort. Radiology 2018;288:600–609.
66. Han MK, Kazerooni EA, Lynch DA, Liu LX, Murray S, Curtis JL, *et al*.; COPDGene Investigators. Chronic obstructive pulmonary disease exacerbations in the COPDGene Study: associated radiologic phenotypes. *Radiology* 2011;261:274–282.
67. Wells JM, Washko GR, Han MK, Abbas N, Nath H, Mamary AJ, *et al*.; COPDGene Investigators; ECLIPSE Study Investigators. Pulmonary arterial enlargement and acute exacerbations of COPD. *N Engl J Med* 2012;367:913–921.
68. Vestbo J, Edwards LD, Scanlon PD, Yates JC, Agusti A, Bakke P, *et al*.; ECLIPSE Investigators. Changes in forced expiratory volume in 1 second over time in COPD. *N Engl J Med* 2011;365: 1184–1192.
69. Tanabe N, Muro S, Tanaka S, Sato S, Oguma T, Kiyokawa H, *et al*. Emphysema distribution and annual changes in pulmonary function in male patients with chronic obstructive pulmonary disease. *Respir Res* 2012;13:31.
70. Hogg JC, Macklem PT, Thurlbeck WM. Site and nature of airway obstruction in chronic obstructive lung disease. *N Engl J Med* 1968; 278:1355–1360.

71. McDonough JE, Yuan R, Suzuki M, Seyednejad N, Elliott WM, Sanchez PG, *et al*. Small-airway obstruction and emphysema in chronic obstructive pulmonary disease. *N Engl J Med* 2011;365: 1567–1575.
72. Rahaghi FN, van Beek EJ, Washko GR. Cardiopulmonary coupling in chronic obstructive pulmonary disease: the role of imaging. *J Thorac Imaging* 2014;29:80–91.
73. Matsuoka S, Washko GR, Yamashiro T, Estepar RS, Diaz A, Silverman EK, *et al*.; National Emphysema Treatment Trial Research Group. Pulmonary hypertension and computed tomography measurement of small pulmonary vessels in severe emphysema. *Am J Respir Crit Care Med* 2010;181:218–225.
74. Estépar RS, Kinney GL, Black-Shinn JL, Bowler RP, Kindlmann GL, Ross JC, *et al*.; COPDGene Study. Computed tomographic measures of pulmonary vascular morphology in smokers and their clinical implications. *Am J Respir Crit Care Med* 2013;188: 231–239.
75. Estépar RS, Ross JC, Krissian K, Schultz T, Washko GR, Kindlmann GL. Computational vascular morphometry for the assessment of pulmonary vascular disease based on scale-space particles. *Proc IEEE Int Symp Biomed Imaging* 2012:1479–1482.
76. Rahaghi FN, Wells JM, Come CE, De La Bruere IA, Bhatt SP, Ross JC, *et al*.; COPDGene Investigators. Arterial and venous pulmonary vascular morphology and their relationship to findings in cardiac magnetic resonance imaging in smokers. *J Comput Assist Tomogr* 2016;40:948–952.
77. Nardelli P, Jimenez-Carretero D, Bermejo-Peláez D, Ledesma-Carbayo MJ, Rahaghi FN, San José Estépar R. Deep-learning strategy for pulmonary artery-vein classification of non-contrast CT images. *Proc IEEE Int Symp Biomed Imaging* 2017:384–387.
78. Bhatt SP, Dransfield MT. Chronic obstructive pulmonary disease and cardiovascular disease. *Transl Res* 2013;162:237–251.
79. Budoff MJ, Nasir K, Kinney GL, Hokanson JE, Barr RG, Steiner R, *et al*. Coronary artery and thoracic calcium on noncontrast thoracic CT scans: comparison of ungated and gated examinations in patients from the COPDGene cohort. *J Cardiovasc Comput Tomogr* 2011;5: 113–118.
80. Kurugol S, San Jose Estepar R, Ross J, Washko GR. Aorta segmentation with a 3D level set approach and quantification of aortic calcifications in non-contrast chest CT. *Conf Proc IEEE Eng Med Biol Soc* 2012;2012: 2343–2346.
81. Kurugol S, Come CE, Diaz AA, Ross JC, Kinney GL, Black-Shinn JL, *et al*. Automated quantitative 3D analysis of aorta size, morphology, and mural calcification distributions. *Med Phys* 2015;42:5467–5478.
82. Rahaghi FN, Vegas-Sanchez-Ferrero G, Minhas JK, Come CE, De La Bruere I, Wells JM, *et al*.; COPDGene Investigators. Ventricular geometry from non-contrast non-ECG-gated CT scans: an imaging marker of cardiopulmonary disease in smokers. *Acad Radiol* 2017; 24:594–602.
83. Bhatt SP, Vegas-Sánchez-Ferrero G, Rahaghi FN, MacLean ES, Gonzalez-Serrano G, Come CE, *et al*. Cardiac morphometry on computed tomography and exacerbation reduction with β-blocker therapy in chronic obstructive pulmonary disease. *Am J Respir Crit Care Med* 2017;196:1484–1488.
84. Diaz AA, Young TP, Kurugol S, Eckbo E, Muralidhar N, Chapman JK, *et al*.; COPDGene investigators. Abdominal visceral adipose tissue is associated with myocardial infarction in patients with COPD. *Chronic Obstr Pulm Dis* 2015;2:8–16.
85. Decramer M, Janssens W. Chronic obstructive pulmonary disease and comorbidities. *Lancet Respir Med* 2013;1:73–83.
86. McDonald ML, Diaz AA, Ross JC, San Jose Estepar R, Zhou L, Regan EA, *et al*. Quantitative computed tomography measures of pectoralis muscle area and disease severity in chronic obstructive pulmonary disease: a cross-sectional study. *Ann Am Thorac Soc* 2014;11: 326–334.
87. Qaseem A, Snow V, Shekelle P, Hopkins R Jr, Forciea MA, Owens DK; Clinical Efficacy Assessment Subcommittee of the American College of Physicians. Screening for osteoporosis in men: a clinical practice guideline from the American College of Physicians. *Ann Intern Med* 2008;148:680–684.
88. Jaramillo JD, Wilson C, Stinson DS, Lynch DA, Bowler RP, Lutz S, *et al*.; COPDGene Investigators. Reduced bone density and vertebral fractures in smokers: men and COPD patients at increased risk. *Ann Am Thorac Soc* 2015;12:648–656.
89. Bermejo-Peláez D, San José Estepar R, Ledesma-Carbayo MJ. Emphysema classification using a multi-view convolutional network. *Proc IEEE Int Symp Biomed Imaging* 2018:519–522.
90. Castaldi PJ, Dy J, Ross J, Chang Y, Washko GR, Curran-Everett D, *et al*. Cluster analysis in the COPDGene study identifies subtypes of smokers with distinct patterns of airway disease and emphysema. *Thorax* 2014;69:415–422.
91. Binder P, Batmanghelich NK, Estepar RS, Golland P. Unsupervised discovery of emphysema subtypes in a large clinical cohort. *Mach Learn Med Imaging* 2016;10019:180–187.
92. Nardelli P, Ross JC, San José Estépar R. CT image enhancement for feature detection and localization. *Lect Notes Comput Sci* 2017; 10434:224–232.
93. Charbonnier JP, Rikxoort EMV, Setio AAA, Schaefer-Prokop CM, Ginneken BV, Ciompi F. Improving airway segmentation in computed tomography using leak detection with convolutional networks. *Med Image Anal* 2017;36:52–60.
94. González G, Ash SY, Vegas-Sánchez-Ferrero G, Onieva Onieva J, Rahaghi FN, Ross JC, *et al*.; COPDGene and ECLIPSE Investigators. Disease staging and prognosis in smokers using deep learning in chest computed tomography. *Am J Respir Crit Care Med* 2018;197: 193–203.
95. Hardin M, Silverman EK. Chronic obstructive pulmonary disease genetics: a review of the past and a look into the future. *Chronic Obstr Pulm Dis* 2014;1:33–46.
96. Cho MH, Castaldi PJ, Hersh CP, Hobbs BD, Barr RG, Tal-Singer R, *et al*.; NETT Genetics, ECLIPSE, and COPDGene Investigators. A genome-wide association study of emphysema and airway quantitative imaging phenotypes. *Am J Respir Crit Care Med* 2015; 192:559–569.
97. Boueiz A, Chang Y, Cho MH, Washko GR, San José Estépar R, Bowler RP, *et al*.; COPDGene Investigators. Lobar emphysema distribution is associated with 5-year radiological disease progression. *Chest* 2018;153:65–76.
98. Castaldi PJ, Cho MH, San José Estépar R, McDonald ML, Laird N, Beaty TH, *et al*.; COPDGene Investigators. Genome-wide association identifies regulatory Loci associated with distinct local histogram emphysema patterns. *Am J Respir Crit Care Med* 2014;190:399–409.
99. Lee JH, Cho MH, Hersh CP, McDonald ML, Wells JM, Dransfield MT, *et al*.; COPDGene and ECLIPSE Investigators. IREB2 and GALC are associated with pulmonary artery enlargement in chronic obstructive pulmonary disease. *Am J Respir Cell Mol Biol* 2015;52:365–376.
100. Diaz AA, Zhou L, Young TP, McDonald ML, Harmouche R, Ross JC, *et al*.; ECLIPSE investigators. Chest CT measures of muscle and adipose tissue in COPD: gender-based differences in content and in relationships with blood biomarkers. *Acad Radiol* 2014;21:1255–1261.